View metadata, citation and similar papers at core.ac.uk

brought to you by CORE

provided by Elsevier - Publisher Connector

Biochimica et Biophysica Acta 1842 (2014) 1423–1432

Contents lists available at ScienceDirect

Biochimica et Biophysica Acta

journal homepage: www.elsevier.com/locate/bbadis

MFAP3L activation promotes colorectal cancer cell invasion and metastasis

Xiaomin Lou [a,1], Bin Kang [a,1], Jun Zhang [a], Chunyi Hao [b], Xiuyun Tian [b], Wenmei Li [b], Ningzhi Xu [c], Youyong Lu [b,*], Siqi Liu [a,**]

[a] CAS Key Laboratory of Genome Sciences and Information, Beijing Institute of Genomics, Chinese Academy of Sciences, No. 1 Beichen West Road, Chaoyang District, Beijing 100101, China

[b] Laboratory of Molecular Oncology, Key Laboratory of Carcinogenesis and Translational Research, Peking University School of Oncology, Beijing Institute for Cancer Research, 52 Fucheng Road, Haidian District, Beijing 100142, China

[c] Laboratory of Cell and Molecular Biology, Cancer Institute and Cancer Hospital, Chinese Academy of Medical Sciences, No. 17 Panjiayuannanli, Chaoyang District, Beijing 100021, China

ARTICLE INFO

Article history:
Received 17 April 2013
Received in revised form 31 March 2014
Accepted 7 April 2014
Available online 13 April 2014

Keywords:
MFAP3L
Protein kinase
Metastasis
Colorectal cancer

ABSTRACT

An abundance of microfibril-associated glycoprotein 3-like (MFAP3L) significantly correlates with distant metastasis in colorectal cancer (CRC), although the mechanism has yet to be explained. In this study, we observed that MFAP3L knock-down resulted in reduced CRC cell invasion and hepatic metastasis. We evaluated the cellular location and biochemical functions of MFAP3L and found that this protein was primarily localized in the nucleus of CRC cells and acted as a protein kinase. When EGFR translocated into the nucleus upon stimulation with EGF, MFAP3L was phosphorylated at Tyr287 within its SH2 motif, and the activated form of MFAP3L phosphorylated ERK2 at Thr185 and Tyr187. Moreover, the metastatic behavior of CRC cells *in vitro* and *in vivo* could be partially explained by activation of the nuclear ERK pathway through MFAP3L phosphorylation. Hence, we experimentally demonstrated for the first time that MFAP3L likely participates in the nuclear signaling of EGFR and ERK2 and acts as a novel nuclear kinase that impacts CRC metastasis.

© 2014 Elsevier B.V. All rights reserved.

1. Introduction

Microfibril-associated protein 3-like (MFAP3L) is a microfibril-associated glycoprotein (MAGP). MAGPs are non-fibrillin, microfibrillar proteins that comprise the structure of microfibrils. It is well accepted that MAGPs bind to distinct regions of fibrillin and facilitate microfibrillar assembly. Although no known human disease is linked directly to MAGP genes, recent evidence has implicated the involvement of MAGPs in tumorigenesis. For instance, several groups observed that MAGP2 (MFAP5) expression is increased in different human cancer tissues and cancer cell lines. In head and neck cancer, high MAGP2 expression is accompanied by poor survival [1]. In ovarian cancer cells, MAGP2 serves as a prognostic indicator of prolonged tumor cell survival and increased endothelial cell motility [2–4]. Thus, MAGPs are thought to promote the acquisition of the vascular phenotype requisite for tumor growth and metastasis, although the detailed mechanisms have not been clearly elucidated.

Our group observed, for the first time, that MFAP3L was up-regulated in primary tumor tissues of colorectal cancer (CRC) patients and that this expression closely correlated with distant metastasis. Based on the results of proteomics and immunohistochemistry analyses, we previously proposed that the protein signature of MFAP3L, phosphorylated IκBα and TNFα could be used as a reference to estimate hepatic metastasis risk in CRC patients [5]. This conclusion was recently confirmed in another study, in which a set of molecular biomarkers, including EGFR, MFAP3L and CapG, exhibited high sensitivity and specificity for predicting colorectal liver metastasis [6]. MFAP3L was first cloned from the human testicular cDNA library, and its abundance in adult testis was found to be ten-fold higher than in embryonic testis [7]. The MFAP3L gene is localized at 4q32.3 and consists of two exons within a 15-kb genomic region. Its full-length mRNA sequence contains 1345 bp, and its protein sequence consists of 409 amino acids. Using cDNA microarrays and Southern blots, Xiao et al. found that the MFAP3L gene is highly expressed in the human testis and prostate and is expressed at a low level in the colon and ovary. In addition, bioinformatic analysis of the MFAP3L gene suggests a single-pass membrane protein with a trans-membrane domain at 150–172 aa, several N-glycosylation sites in the extracellular region and a cluster of proximal phosphorylation sites, which are similar to kinases such as tyrosine kinases, PKC and casein kinase II [7]. There is also a conserved SH2 motif at 279–294 aa that contains a potential EGFR phosphorylation site (NetphosK 1.0 Server). The proximity of this potential phosphorylation

* Corresponding author. Tel.: +86 10 8819 6765; fax: +86 10 8812 2437.
** Correspondence to: S. Liu, Beijing Institute of Genomics, Chinese Academy of Sciences, No. 1 Beichen West Road, Chaoyang District, Beijing 100101, China . Tel./fax: +86 10 8409 7465.
E-mail addresses: yongylu@public.bta.net.cn (Y. Lu), siqiliu@big.ac.cn (S. Liu).
[1] These authors contributed equally to this work.

http://dx.doi.org/10.1016/j.bbadis.2014.04.006
0925-4439/© 2014 Elsevier B.V. All rights reserved.

sites implies that MFAP3L may act as a protein kinase involved in the EGFR signaling pathway.

It is well known that EGF-induced signaling is associated with tumor invasion and metastasis [8]. Its receptor, EGFR, is a typical protein tyrosine kinase, and activated EGFR phosphorylates downstream proteins containing SH2-domains, leading to cascading effects on several signaling pathways and more aggressive tumor cell behaviors [9]. The ligand-dependent nuclear translocation of EGFR has recently been detected in various cancer cells and clinical cases [10,11]. In addition, the accumulation of nuclear EGFR, especially its phosphorylated form, closely correlates with poor clinical outcomes, such as advanced TNM stage, metastasis and limited postoperative survival [12,13]. Because there is a positive correlation between MFAP3L abundance and CRC metastasis, and MFAP3L contains a conserved SH2 motif that is potentially targeted by EGFR, we sought to determine whether the phosphorylation status of MFAP3L acts as a regulatory factor of CRC metastasis.

To explore the biological functions and mechanisms of MFAP3L involved in cancer metastasis, we first adopted an RNAi technique to verify MFAP3L involvement in CRC invasion and metastasis. We then investigated MFAP3L cellular localization and whether it exhibited kinase activity *in vivo*. Based on confocal microscopy and immunoblotting experiments, MFAP3L was shown to be primarily localized in the nucleus and to act as a substrate of nuclear-translocated EGFR. Furthermore, activated MFAP3L served as a kinase that phosphorylated ERK2 at Tyr187. MFAP3L over-expression triggered the ERK cascade, which promoted the expression of ERK-regulated genes and augmented colon cancer cell metastasis and invasion. Thus, our results demonstrate that MFAP3L is an active element of the nuclear EGFR signaling pathway and the process of CRC metastasis.

2. Materials and methods

2.1. Materials and antibodies

A total of 57 colorectal carcinoma samples were collected at the Beijing Cancer Hospital, Beijing, China. Carcinoma samples were obtained from the core tumor focus, and matched normal adjacent samples were collected 5 cm away from the tumor tissues. The macroscopic pathological features and microscopic histological classifications were reviewed by a senior pathologist. All tissue samples were approved for research projects by the Research Ethical Committee of Beijing Cancer Hospital. EGF, AG1478, U0126, myelin basic protein (MBP; bovine) and a protease inhibitor cocktail were purchased from Sigma. The following antibodies were purchased from Santa Cruz: EGFR; MEK1; ERK2; cathepsin D; MMP2; osteopontin, actin; lamin A; aldehyde reductase (AR); phosphorylated EGFR (Tyr1045); phosphorylated ERK (Tyr204); and p-Tyr (PY99). The following antibodies were purchased from SAB: cMyc-tag; ELK1; phosphorylated ELK1 (Ser389); and phosphorylated ERK (Thr202). The polyclonal antibody targeting phosphorylated MFAP3L (Tyr287) is commercially available through SAB. To obtain the polyclonal antibody for MFAP3L, we immunized rabbits with recombinant truncated MFAP3L protein, which contained the N-terminal 103 amino acids. SW480, SW620 and CHO cells were obtained from the American Type Culture Collection (ATCC). Cells were maintained in Dulbecco's modified Eagle's medium containing 100 U/mL penicillin, 100 mg/mL streptomycin and 10% FBS.

2.2. Molecular cloning and plasmid construction

The full-length CDS regions of human MFAP3L, ERK2 and EGFR were amplified by PCR from the cDNA library of the human testis. The intracellular domain (669–1210) of EGFR (EGFR-ICD) was amplified using the template for full-length EGFR, and all fragments were cloned into the pcDNA3.1/myc-His vector. The dominant-positive (DP; Y287D) and dominant-negative (DN; Y287A) mutants of MFAP3L, the pNLS mutant (RRR669-671AAA) of EGFR and the dominant-negative mutant (Y187F) of ERK2 were generated using a QuikChange Site-Directed Mutagenesis Kit (Stratagene). His-tagged recombinant proteins of wild-type and mutant MFAP3L and ERK2, as well as EGFR-ICD, were expressed in *Escherichia coli* BL21 DE3 cells using the pET28a vector and purified by Ni-affinity chromatography. The digestion sites for the expression vectors for MFAP3L, EGFR and ERK2 were as follows: *Bam*HI/*Hind* III, *Nhe*I/*Hind* III and *Nde*I/*Xho*I, respectively. The specific RNAi vectors for MFAP3L and ERK2 were constructed using p*Silencer*™ 3.1-H1 neo (Life Technologies). The target DNA sequences for MFAP3L were 5′-GCATCTACGGCACCGTGAAC-3′ and 5′-GGCATTTG AGATCGCCAAG-3′ and for ERK2 was 5′-GGAAAAGCTCAAAGAACTA-3′; these sequences have previously been verified [14].

2.3. Cell transfection

Two colon cancer cell lines, SW480 and SW620, were cultured in complete DMEM (Invitrogen) containing 10% fetal bovine serum (FBS; Thermo Fisher), penicillin (100 kU/L) and streptomycin (100 mg/L) at 37 °C in a humidified atmosphere containing 5% CO_2. A Chinese hamster ovary cell line (CHO) was cultured in F12 medium (Invitrogen) containing 5% FBS (Thermo Fisher) at 37 °C in a humidified atmosphere containing 5% CO_2. All transfections were performed using Lipofectamine 2000 (Invitrogen), and empty vectors were transfected as negative controls. For transient transfection, the cells were harvested after 24–48 h for use in subsequent experiments. For the selection of stable cells, following a 1-month selection period using 600 μg/ml G418, the existing clones were examined through western blot analyses.

2.4. MTT, scratch wound healing and Transwell invasion assays

Cell proliferation was measured using the 3-(4,5-dimethylthiazolyl-2)-2,5-diphenyltetrazolium bromide (MTT) assay. Approximately 2000 cells were plated in each well of a 96-well plate and grown for 0, 1, 2 or 3 days. At 4 h before the end of the incubation, 10 μL of MTT (5 mg/mL) was added to each well followed by 100 μL of DMSO, and the samples were mixed to dissolve the crystals. The reaction products were detected using a spectrometer at 570/630 nm. The result of each time point represented three independent replicates. Cell migration was examined using the scratch wound healing assay. Cells were grown to confluence in 60-mm culture dishes. A sterile pipette tip was used to scratch a 1-mm-wide wound along the center of the dish, and the demarcated wound area was imaged using an inverted Nikon microscope at various times after wounding (0, 12 and 24 h). Cell invasion was detected using Transwell invasion assay. Twenty-five thousand cells were suspended in a culture medium without serum and plated in the upper chambers (BD BioCoat™ Matrigel Invasion Chambers in 24-well plates, BD Biosciences), and the bottom wells were filled with NIH3T3 cell culture medium. After 24 h, the inserts were washed with PBS, the non-migratory cells were removed with cotton swabs, and the filters were collected for HE staining. Ten fields of view were counted under an inverted Nikon microscope, and, for each cell type, three independent experiments were performed to calculate the average number of stained cells.

2.5. Hepatic metastasis model in nude mice

The tested cells were suspended in Hank's solution, and 2×10^6 cells were injected into the spleens of 5-week old female BalB/c nude mice. The mice were anesthetized and placed on their right sides, and their spleens were exposed through a 5–7 mm cut on the left flank. Cells were injected into the middle of the spleen using a tuberculin syringe with a 26G needle. The mice were maintained according to the guidelines of the National Institutes of Health for the Care and Use of Laboratory Animals. The mice were sacrificed 7 weeks after the operation, and the liver and spleen tissues were evaluated through necropsy.

2.6. Cellular fractionation and western blot analysis

Cells were washed with pre-chilled PBS and homogenized in buffer containing 210 mM sucrose, 70 mM mannitol, 1 mM EDTA, 1 mM PMSF, 1.5 mM $MgCl_2$ and 10 mM HEPES. Nuclear and non-nuclear fractions were prepared with differential centrifugation. Nuclei were pelleted at 1000 ×*g* for 10 min, and the non-nuclear fraction was obtained after centrifugation at 16,000 ×*g* for 10 min as a supernatant. The sample was lysed in buffer containing 8 M urea, 4% CHAPS, 0.5% Pharmalyte (pH 3–10 L, GE), 10 mM DTT, 1 mM PMSF and 2 mM EDTA. The lysate was electrophoresed using SDS-PAGE and electrotransferred onto a PVDF membrane. The PVDF membrane was incubated with antibodies and visualized with an ECL kit using the ImageQuant ECL system (Bio-Rad).

2.7. Immunofluorescence and confocal microscopy

Cells were fixed with 3.7% formaldehyde for 15 min and permeabilized with 0.2% Triton X-100 for 6 min. PBS containing 1% BSA was incubated with the cells for 1 h at room temperature to block non-specific binding, and primary antibodies at a dilution of 1:100 in blocking buffer were incubated with the cells for 2 h. After thorough washing with 0.05% Triton X-100 in PBS, the cells were incubated with the appropriate FITC-conjugated secondary antibodies at a dilution of 1:100 in blocking buffer for 1 h. Fluorescent images were acquired using a confocal laser-scanning microscope (Zeiss LSM510) and analyzed with the LSM5 Image Browser program (Carl Zeiss Micro-Imaging). For a reference of organelle localization, DAPI was used to stain the nucleus.

2.8. Immunohistochemical staining

The colorectal carcinoma and matched normal samples for immunohistochemical (IHC) staining were collected at the Beijing Cancer Hospital in Beijing, China. The carcinoma samples were obtained from the core tumor focus, and the matched normal samples were collected 5 cm away from the tumor tissues. IHC staining was performed using an EnVision™+ Kit (Dako). The tissue slices were incubated with the primary antibody against MFAP3L at a dilution of 1:50 overnight at 4 °C. In the negative control group, 1% bovine serum albumin was used instead of the primary antibody.

2.9. Immunoprecipitation

Whole cell and nuclear lysates were prepared in lysis buffer containing 50 mM HEPES (pH 7.4), 150 mM NaCl, 1% NP40, 1 mM EDTA, 10% glycerol and 2% protease inhibitor cocktail. One milligram of each lysate was precleared by incubation of protein A beads bound with pre-serum for 2 h. After centrifugation at 1000 ×*g* for 5 min, the supernatants were transferred to the slurry containing 2 μg of antibody and protein A beads for overnight incubation. After thorough washing with lysis buffer, the immunoprecipitated complexes bound to the protein A beads were dissolved in SDS loading buffer and detected by western blot analysis or LC MS/MS.

2.10. Pull-down assay

One milligram of whole cell or nuclear lysate was prepared in lysis buffer containing 50 mM HEPES (pH 7.4), 100 mM NaCl, 1% NP40, 25 mM imidazole, 1 mM EDTA, 10% glycerol and 2% protease inhibitor cocktail and precleared by incubation with Ni-NTA beads for 2 h. After centrifugation at 500 ×*g* for 5 min, the supernatants were incubated with 40 mg of recombinant MFAP3L protein and Ni-NTA beads overnight. After thorough washing with lysis buffer, the protein complexes were dissolved in SDS loading buffer and detected by western blot analysis.

2.11. In vitro kinase assay

Five micrograms of recombinant MFAP3L or MBP protein, 1 μg of recombinant ERK2, or the product precipitated by the cMyc-tag or MFAP3L antibody was incubated with 0.5 μg of recombinant ERK2 in 20 μL of kinase assay buffer containing 50 mM Tris (pH 7.5), 10 mM $MgCl_2$, 1 mM DTT, 0.1 mM sodium orthovanadate, 40 μg/mL PS, 30 μg/mL DAG and 0.1 mM unlabeled ATP for 30 min at 30 °C. The reaction was halted by the addition of SDS loading buffer, and the phosphorylation status was detected by autoradioactivity (6 h at −80 °C) or western blot analysis.

2.12. Identification of phosphorylation sites using mass spectrometry

To identify the phosphorylation sites of the substrates, the corresponding bands on SDS-PAGE gels were manually excised and subjected to in-gel digestion with trypsin (Promega) at 37 °C overnight. The digested products were identified by LC MS/MS using an UltiMate 3000 Nano HPLC system (Dionex) and a three-dimensional high-capacity ion trap mass spectrometer (Esquire HCTplus, Bruker Daltonics). MASCOT-compatible files were created using Data Analysis 3.3 software (Bruker Daltonics), and searches were performed using MASCOT software (version 2.2.04, Matrix Science) with the latest human or bovine NCBI database. All searches were performed with tryptic specificity, allowing for one missed cleavage. Oxidation of methionine and phosphorylation of tyrosine, serine and threonine were considered variable modifications. MS2 spectra acquired with the ion trap instrument were generally accepted with a MASCOT cutoff score of 20 and a mass tolerance of 0.4 Da for the MS and MS2 experiments. Additionally, the identification results were reproducible across parallel injections as well as sample preparations.

2.13. Statistical analyses

The SPSS 14.0 software was used for statistical analyses (SPSS, Chicago, IL, USA). Student's *t*-test was used to compare the values between subgroups, and $p < 0.05$ was considered to represent a significant difference between groups of data.

3. Results

3.1. MFAP3L knock-down inhibits CRC cell metastasis

MFAP3L expression levels correlate with CRC distant metastasis according to a previous report using a proteomic survey [5]. In the present study, we first attempted to identify whether CRC metastasis was associated with changes in MFAP3L abundance in cancer cells. Two different RNAi sequences targeting MFAP3L, 5′-GCATCTACGGCACCGTGAAC-3′ and 5′-GGCATTTGAGATCGCCAAG-3′, were cloned into p*Sliencer*™ 3.1-H1 neo, designated as pSi1 and pSi2, respectively. These two RNAi vectors were then transfected into SW620 colon cancer cells, which demonstrate a high metastatic potential, and stable cell lines were selected. Fig. 1a shows that the knock-down effect of pSi2 was more efficient than that of pSi1. Thus, pSi2 SW620 cells, designated as MF−, were used for the following experiments. Compared with control SW620 cells transfected with the non-targeting (NT) construct, the MF− cells exhibited a clear reduction in growth rate as measured by the MTT assay (Fig. 1b). In addition, migration and invasion, as indicated by the scratch wound healing and Transwell assays, respectively, of MF− cells were reduced compared with NT cells (Fig. 1c and d, $p < 0.001$). Furthermore, we employed a commonly accepted mouse model to study hepatic metastasis *in vivo* by injecting MF− or NT cells into the spleens of nude mice (7 mice/group) and monitoring the frequency of liver metastasis based on tumor formation in the liver. In the NT group, 4 mice developed splenic tumors (57%), and 5 developed hepatic metastasis (71%), while in the MF− group, 2 mice developed splenic tumors (29%), and none acquired hepatic metastasis

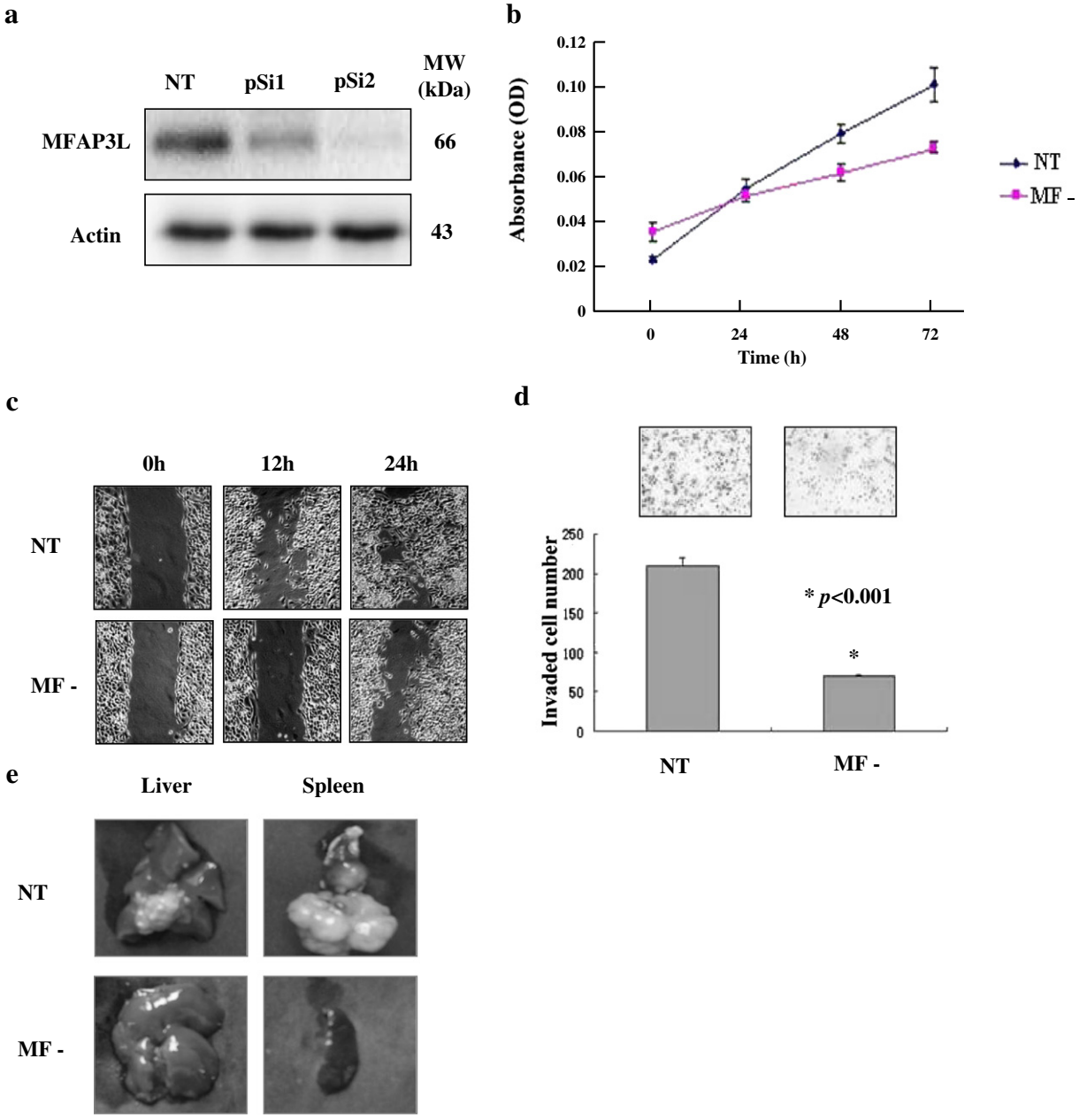

Fig. 1. *MFAP3L knock-down inhibits colon cancer cell metastasis.* a, MFAP3L knock-down in SW620 cells. NT, pSi1 and pSi2 indicate the empty vector and two different RNAi vectors, respectively. Western blot analysis was performed to detect the effect of RNAi. b–d, MFAP3L knock-down reduced the growth, migration and invasion capabilities of SW620 cells. MTT, scratch wound healing (SWH) and Transwell invasion assays were performed using MFAP3L knock-down cells (MF−) and control cells (NT). For the MTT assay, the result of each time point represents three replicates. For the SWH assay, five fields of view for each cell line were observed, and a representative view is shown. For the Transwell assay, ten views were counted, and three independent experiments were performed to calculate the average. All above tests were conducted in triple bio-replication. e, MFAP3L knock-down inhibited tumorigenesis and hepatic metastasis in SW620 cells. Seven mice were injected with either NT or MF− cells; representative images of splenic tumorigenesis and hepatic metastasis are shown.

(0%; Fig. 1e). These data indicate that MFAP3L likely participates in the regulation of CRC metastasis.

3.2. MFAP3L is mainly localized in the nucleus

To elucidate how MFAP3L participates in CRC metastasis, we sought to determine MFAP3L localization within cellular organelles. Cells stably overexpressing MFAP3L were established through transfection of pcDNA3.1-MFAP3L-myc-His into SW480 cells, denoted as MF+ cells, and the empty vector was transfected into SW480 cells, denoted as EV+ cells. The images acquired from confocal microscopy indicated that MFAP3L primarily accumulated in the nucleus and was slightly distributed in the cytoplasm and plasma membrane (Fig. 2a). A similar result was observed in CHO cells (Fig. 3e). MFAP3L localization was also examined in MF+ cells through cellular fractionation and western blot analysis. As illustrated in Fig. 2b, MFAP3L was strongly immunorecognized in the nuclear fraction, whereas it was only slightly detected in the non-nuclear fraction. Moreover, the nuclear localization of MFAP3L was observed in the IHC images of 57 CRC tissues and their normal adjacent tissues. The nuclear localization of MFAP3L was detected in almost 80% of the CRC tissues showing positive MFAP3L staining (24 out of 31 cases, Fig. 2c) and could not be observed in 5 normal adjacent samples showing positive MFAP3L staining. Nuclear-localized MFAP3L was also more significantly expressed in CRC tissues compared

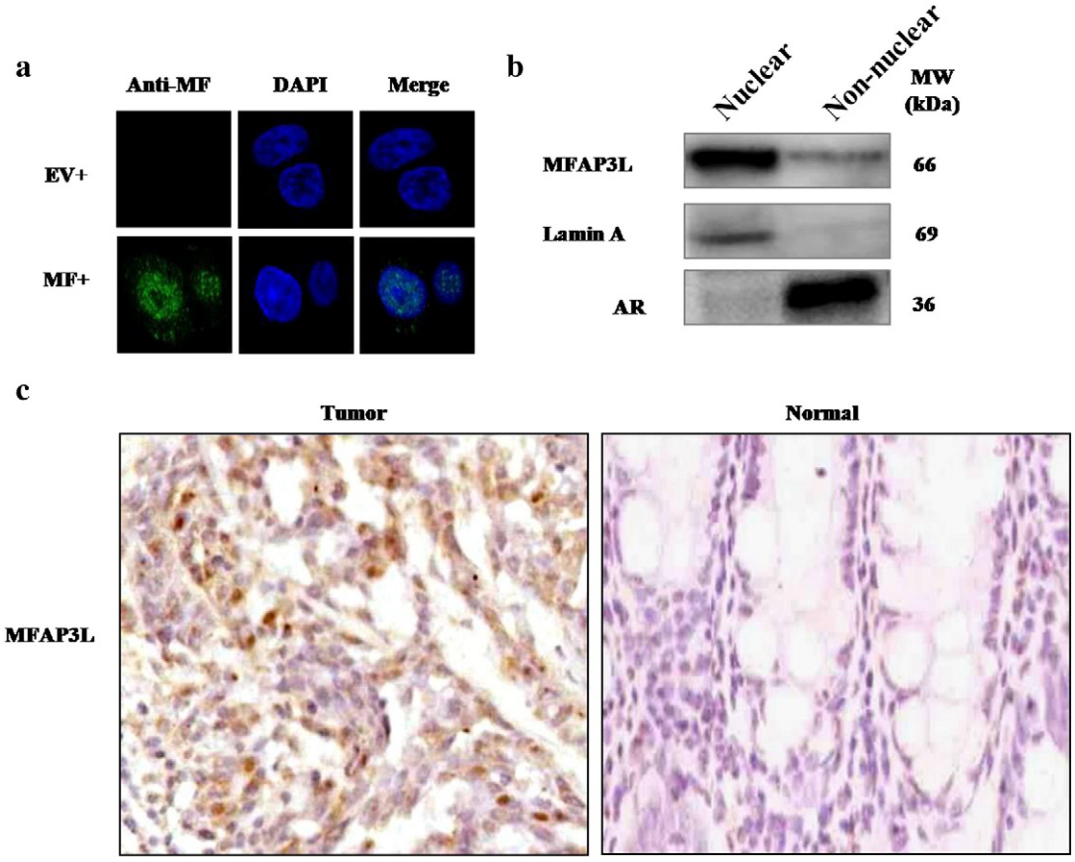

Fig. 2. *MFAP3L is mainly localized in the nucleus.* a–b, The majority of MFAP3L protein was localized in the nucleus. Immunofluorescence (IF) and nuclear fractionation (NF) assays were performed to detect MFAP3L localization in MFAP3L-overexpressing SW480 cells (MF+) and control cells (EV+). DAPI staining was used to mark the nucleus in the IF assay, and Lamin A and AR were used as indicators of the nucleus and cytosol, respectively, in the NF assay. c, MFAP3L showed nuclear localization in human CRC tissue samples. IHC staining was performed to detect MFAP3L localization in human CRC tissues and matched normal samples.

with the paired adjacent tissues ($p = 0.00033$, *t*-test). Together, the IHC results were in good agreement with our previous observations and suggested that MFAP3L was likely distributed in the nucleus *in vivo*. Therefore, we concluded that MFAP3L is a predominantly nuclear protein.

3.3. Nuclear translocation of EGFR directly phosphorylates MFAP3L at Tyr287

MFAP3L contains a potential EGFR phosphorylation site. Experimentally, MFAP3L was found to be primarily localized in the nucleus, and EGFR is generally found to be translocated to the nucleus in cancer cells. We thus sought to examine whether nuclear MFAP3L is a target of nuclear-translocated EGFR. To address this question, we first treated MF+ cells with EGF and collected nuclear and non-nuclear fractions at different times after EGF stimulation. As shown in Fig. 3a, both EGFR and phosphorylated EGFR in the nuclear fraction were greatly increased within 1 h of EGF induction, indicating that EGFR nuclear translocation occurred in MF+ cells. Utilizing an *in vitro* kinase assay, we sought to determine whether EGFR directly reacted with MFAP3L. Western blot analysis (Fig. 3b) revealed that the truncated recombinant EGFR with its intracellular domain (ICD) specifically phosphorylated MFAP3L, while the MS spectrum (Fig. 3b) demonstrated that Tyr287 of MFAP3L was phosphorylated by EGFR. We further generated a dominant-negative mutant of MFAP3L (DN; Y287A) and examined its phosphorylation status in the presence of EGFR. The data presented in Fig. 3b revealed no phosphorylation of Tyr287 in DN cells, suggesting that Tyr287 of MFAP3L was an accessible site for EGFR phosphorylation. We next addressed whether EGFR could phosphorylate MFAP3L *in vivo* by treating MF+ and EV+ cells with EGF and monitoring the phosphorylation status of MFAP3L by western blot analysis using an antibody against pTyr287 of MFAP3L at various intervals following EGF treatment. As shown in Fig. 3c, in EV+ cells with a low level of MFAP3L expression, pTyr287 of MFAP3L was almost undetectable, whereas in MF+ cells with a high level of MFAP3L expression, pMFAP3L was clearly enhanced after a 1-h EGF treatment. In addition, a faint pMFAP3L signal could be detected in MF+ cells even without EGF treatment, implying that there were other endogenous kinases that phosphorylated MFAP3L. This result suggested that the phosphorylation of MFAP3L by EGFR *in vivo* was in good agreement with its observed behavior *in vitro*. To confirm EGFR-mediated phosphorylation of MFAP3L, we performed experiments with AG1478, a specific EGFR tyrosine kinase inhibitor. As shown in Fig. 3d, AG1478 treatment clearly inhibited the increased pTyr287 levels of MFAP3L in MF+ cells after a 1-h stimulation with EGF, which indicated that MFAP3L was phosphorylated by EGFR in these cells.

In contrast to SW480 cells, which possess a lower abundance of MFAP3L protein and a higher abundance of EGFR protein, we selected CHO cells, which demonstrate low constitutive EGFR expression and high endogenous MFAP3L expression, to address whether nuclear-translocated EGFR was capable of phosphorylating MFAP3L *in vivo*. We established CHO cells that stably over-expressed wild-type EGFR (EGFR+) or an EGFR mutant (pNLS+), which lacked a nuclear localization signal (RRR669-671AAA) [15]. Upon EGF treatment, wild-type EGFR translocated to the nucleus, whereas no nuclear translocation of pNLS+ was detected (Fig. 3e). Importantly, the two forms of EGFR maintained a similar tyrosine phosphorylation status under EGF treatment, indicating that the two EGFRs shared comparable kinase activities. As shown in Fig. 3f, pTyr287 of MFAP3L was only up-regulated in EGFR+ but not pNLS+ cells, convincingly demonstrating that nuclear-translocated EGFR could phosphorylate MFAP3L *in vivo*.

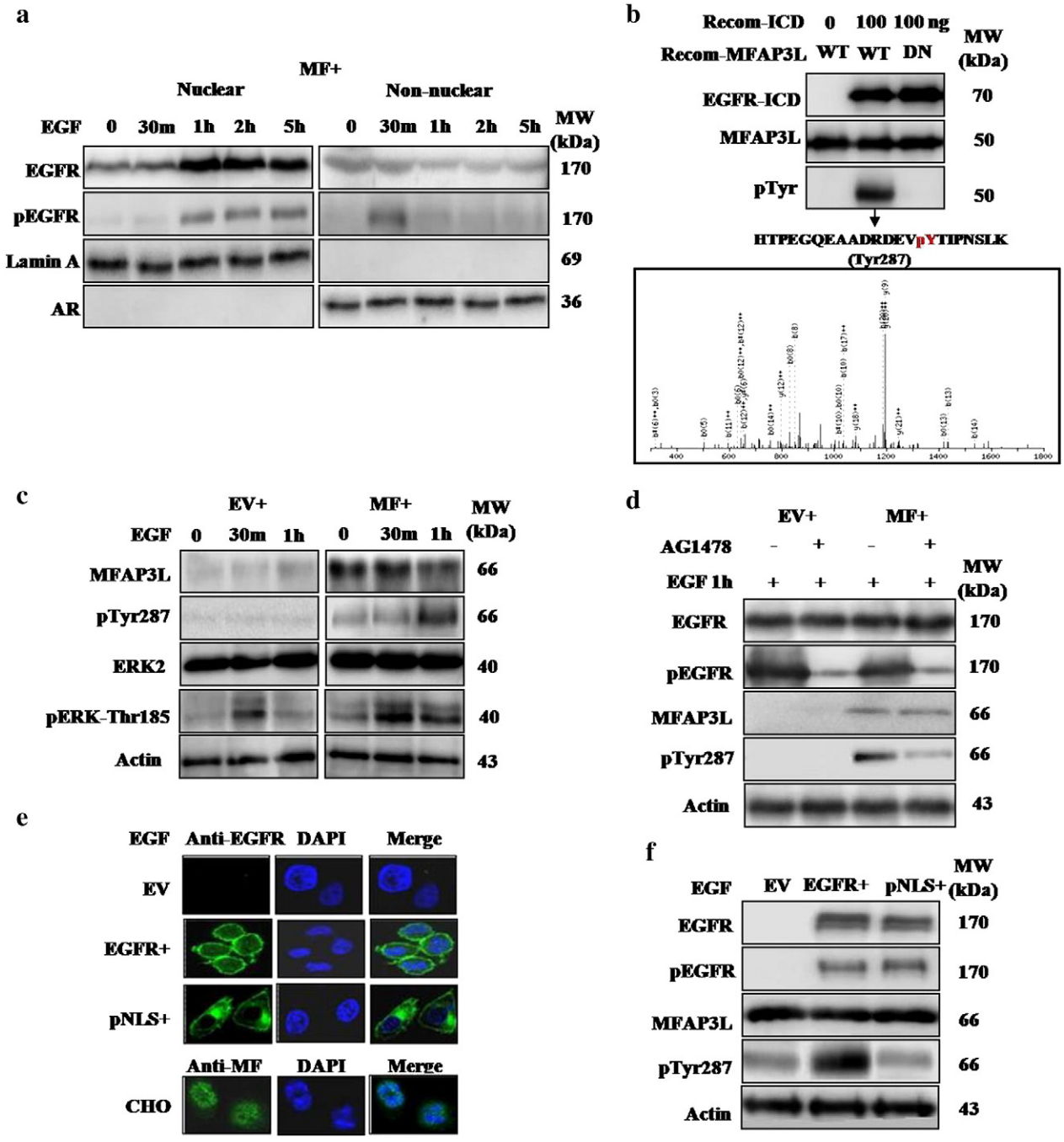

Fig. 3. *EGFR phosphorylates MFAP3L through nuclear translocation.* a, EGFR phosphorylation and nuclear translocation were enhanced upon EGF treatment in MF+ cells. The nuclear and non-nuclear fractions of MF+ cells treated with 100 ng/ml EGF for 1 h were collected for western blot analysis to detect EGFR translocation and phosphorylation status. The time points of EGF treatment were 0, 30 min, 1 h, 2 h and 5 h. Lamin A and AR were used as markers of the nucleus and cytosol, respectively. b, EGFR directly phosphorylated MFAP3L at Tyr287. An *in vitro* kinase assay was performed by incubating 100 ng of the recombinant intracellular domain (ICD) of EGFR with 1 μg of the WT or DN mutant of MFAP3L. MFAP3L phosphorylation was detected using the pTyr antibody, and the phosphorylation site was identified by LC MS/MS. c, Western blot analysis of pTyr287 of MFAP3L and pERK2 in EV+ and MF+ cells treated with EGF (100 ng/mL). The time points included 0, 30 min and 1 h. d, Western blot analysis was used to determine the effect of an EGFR inhibitor on pTyr287 of MFAP3L. pEGFR was detected using an antibody against pTyr1045 of EGFR. AG1478 was used to pretreat the cells at 10 μM for 1 h, and then EGF (100 ng/mL) was added for an additional 1 h. All cells treated with EGF and/or AG1478 were starved in serum-free medium for 24 h, and water and DMSO were added as mock controls for EGF and AG1478 treatment, respectively. e, The localization of EGFR and MFAP3L in CHO cells expressing wild-type (EGFR+) and a mutant lacking the nuclear localization signal (pNLS+) of EGFR. An immunofluorescence assay was performed to detect the distributions of EGFR and MFAP3L in the cells. All cells were treated with EGF for 1 h. f, pTyr287 of MFAP3L was enhanced only when EGFR accumulated in the nucleus. Western blot analysis was performed to determine the phosphorylation levels of EGFR and MFAP3L in EGFR+, pNLS + and EV cells treated with EGF for 1 h.

3.4. MFAP3L binds and phosphorylates ERK2 in the nucleus

Bioinformatic analysis revealed that MFAP3L possesses a glycine-rich stretch of residues in the vicinity of the lysine residue in the N-terminus (98–101 aa) and aspartic acid residues in the central region (282–284, 302–304, 332–333 aa), which are the common features of the catalytic domain of protein kinases. To determine whether there was any measurable protein kinase activity for MFAP3L, we designed two experiments to identify the binding proteins of MFAP3L *in vivo* and to specifically examine its substrate affinity. The proteins that bound to MFAP3L in the nucleus of MF+ cells were enriched through IP using the cMyc-tag antibody followed by protein identification with

LC MS/MS (Fig. 4a). Based on our stringent criterion, a total of six unique proteins were identified that could be localized in or translocated to the nucleus (Table 1). Of these candidate substrates, ERK2, a member of MAP kinase family, is commonly reported to be involved in tumorigenesis and metastasis. We further confirmed the specific interaction between MFAP3L and ERK2 using another approach, whereby the

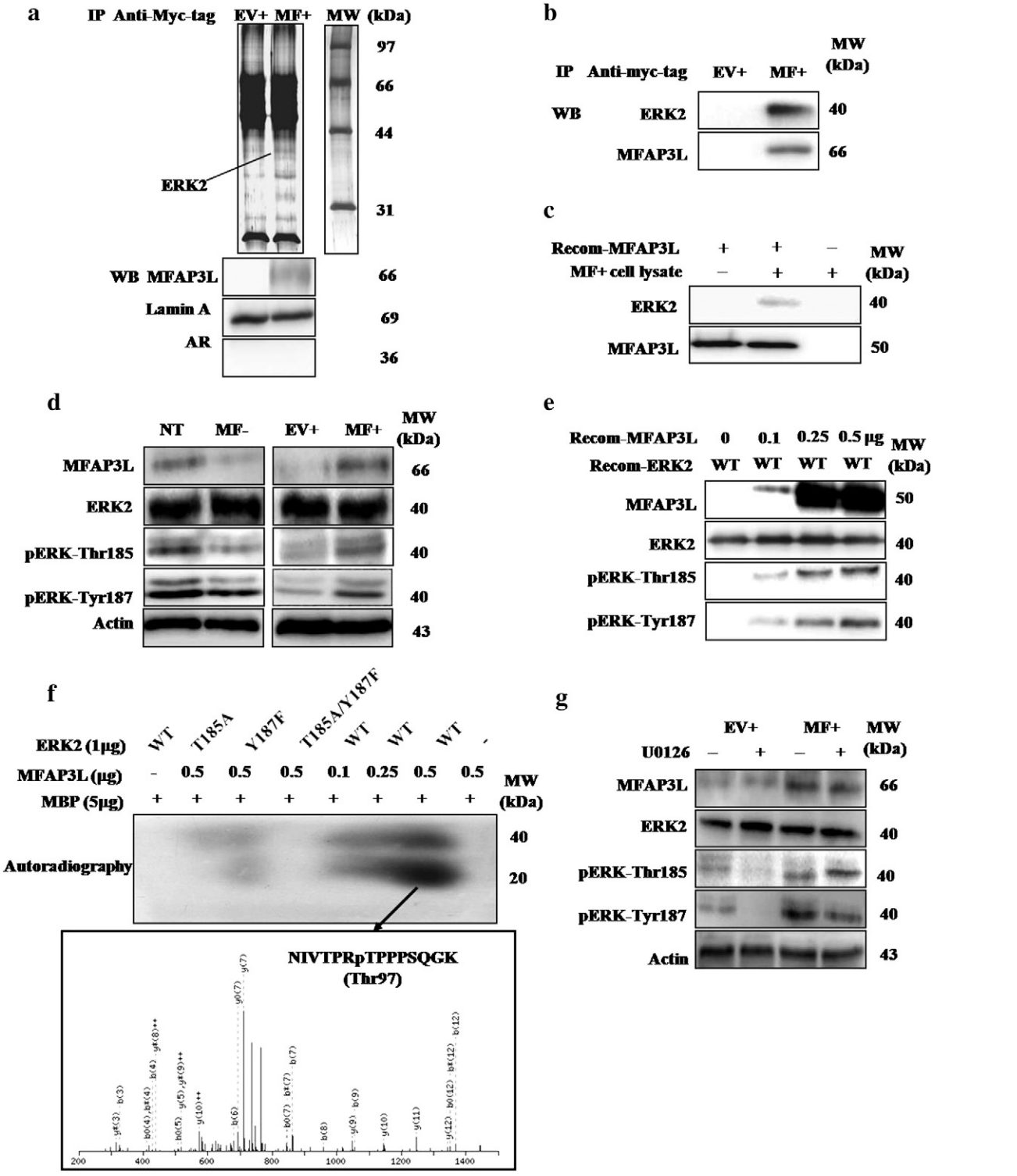

Fig. 4. *MFAP3L binds and phosphorylates ERK2 at Tyr187 in the nucleus.* a, An IP assay using an anti-myc-tag antibody was performed using the nuclear extracts of MF + and EV + cells. The proteins bound to MFAP3L were identified by LC MS/MS. b-c, MFAP3L was found to bind to ERK2 in the nucleus. b, An MFAP3L IP was performed using an anti-myc-tag antibody for the nuclear extracts of MF + and EV + cells. c, A pull-down assay was performed using 40 mg of recombinant His-tagged MFAP3L with SW480 cell nuclear extracts. d, Knock-down and over-expression of MFAP3L reduced and enhanced the phosphorylation of ERK at Thr 185 and Tyr187, respectively. MF +, EV +, MF − and NT cells were used for western blot analysis. e, *In vitro* kinase assay of MFAP3L with wild-type (WT) ERK2. Different amounts of recombinant MFAP3L were analyzed for their effect on ERK2 phosphorylation (1 μg). f, *In vitro* kinase assay of MFAP3L with WT ERK2 and dominant-negative mutants (T185A, Y187F and T185A/Y187F) of ERK2 and its substrate bovine MBP. The phosphorylation of ERK2 (1 μg; 40 kDa) and MBP (5 μg; 20 kDa) was detected through autoradiography after protein separation on a 15% SDS-PAGE gel, and the phosphorylation site of MBP was identified by LC MS/MS. g, ERK2 phosphorylation by MFAP3L was independent of the MEK pathway. The MEK inhibitor U0126 (12.5 μM) was used to treat MF + and EV + cells for 24 h, and the cell lysates were harvested for western blot analysis.

Table 1
The binding proteins of MFAP3L identified by LC MS/MS.

Description	Accession No.	pI	MW	Identified peptides	Nuclear localization	Function annotation
Nup93	gi|116242684	5.5	94	NADKVLELMNK, LVPLNQESVEER	Y	Component of the nucleoporin complex
Lamin A/C	gi|119573381	9.0	79	RTPTPSSLCPSTR, LLEGEEERLR	Y	Components of the nuclear envelope
NONO	gi|34932414	9.0	54	LFVGNLPPDITEEEMRK, FGQAATMEGIGAIGGTPPAFNR	Y	DNA and RNA binding protein
Paraneoplastic 62 kDa antigen	gi|119609629	6.4	47	MYSTNEEQVQEIEYLTK, IHGLTETIER	Y	Nuclear protein binding
ERK2	gi|228860	6.7	40	FRHENIIGINDIIR, YTNLSYIGEGAYGMVCSAYDNVNK	Translocation from cytosol	MAP kinase activity
Histone H2A NDEELNKLLGK	gi|12654707 Y	11.1 Core component of nucleosome	14	VGAGAPVYLAAVLEYLTAEILELAGNAAR		

complexes that were enriched by IP and His pull-down in MF+ cells were analyzed by western blot using appropriate antibodies. In the anti-cMyc IP product, immune-recognition signals for MFAP3L and ERK2 were detected in MF+ cells, but not in EV+ cells, while in the His-MFAP3L pull-down product, a positive immune-recognition signal for ERK2 was found (Fig. 4b and c). Hence, these results were in agreement with our conclusions drawn from the MS data.

It is well known that the biological functions of ERK2 mainly rely on its phosphorylation status and nuclear translocation, although ERK2 has not yet been reported as the substrate of a nuclear kinase. In addition, the complete activation of ERK2 requires its phosphorylation at both Thr185 and Tyr187 in its TXY motif [16]. To determine whether MFAP3L can phosphorylate ERK2, we used two antibodies that specifically recognize pThr185 and pTyr187 of ERK2 to monitor the phosphorylation status of ERK2 *in vivo*. As depicted in Fig. 4d, the two phosphorylation events of ERK2 at Thr185 and Tyr187 were clearly attenuated in MF− cells compared with NT cells, and these events were clearly enhanced in MF+ cells compared to EV+ cells, suggesting that the level of MFAP3L correlated with ERK2 phosphorylation at Thr185 and Tyr187. We then explored whether MFAP3L could directly catalyze ERK2 phosphorylation. In an *in vitro* experiment, we generated the following recombinant proteins: MFAP3L; wild-type (WT) ERK2; and the dominant-negative mutants (T185A, Y187F and T185A/Y187F) of ERK2. The western blot images shown in Fig. 4e and the autoradiography data shown in Fig. 4f (Lanes 5–7) revealed that the phosphorylation levels of ERK2 at Thr185 and Tyr187 were proportional to the concentration of MFAP3L in the reaction mixtures. Fig. 4f (Lanes 2–4) shows that ERK2 phosphorylation was clearly reduced in the mutants T185A and Y187F and completely lost in double mutant (T185A/Y187F). These results demonstrated that MFAP3L could phosphorylate ERK2 at Thr185 and Tyr187.

To further address whether MFAP3L activates ERK2, bovine myelin basic protein (MBP), a common substrate of ERK2, was incorporated into the kinase assay. Fig. 4f (Lanes 5–7) revealed that the phosphorylation status of MBP was proportional to the MFAP3L concentration and the extent of ERK2 phosphorylation. In addition, the phosphorylation of MBP at Thr97, a common site phosphorylated by ERK2, was identified through LC MS/MS (Fig. 4f) [17]. Furthermore, MBP phosphorylation was clearly decreased with the Y187F mutant and completely lost with the T185A and T185A/Y187F mutants (Fig. 4f, Lanes 2–4). These data suggested that the phosphorylation of ERK2 at Thr185 catalyzed by MFAP3L could activate this kinase, while phosphorylation at Tyr187 was required for a higher level of activation. This observation was generally in agreement with a previous report concerning ERK2 activation [16], and these results led us to conclude that MFAP3L acts as a dual kinase that can directly phosphorylate ERK2.

ERK2 activation is generally regulated by the cytoplasmic MEK pathway [18]. To determine whether the MEK pathway impacts the phosphorylation of ERK2 by MFAP3L, we used U0126, a specific MEK inhibitor, to examine the function of MFAP3L as a kinase in the absence of MEK pathway activity. When MF+ and EV+ cells were treated with U0126 for 24 h, pERK2 expression was completely lost in EV+ cells, whereas pERK2 appeared consistently in MF+ cells (Fig. 4g). These results suggest that the kinase activity of MFAP3L is independent of the cytoplasmic MEK pathway.

3.5. MFAP3L activates the ERK2 cascade and enhances colon cancer cell invasion

Because nuclear ERK2 could be phosphorylated by MFAP3L, we next inquired whether the ERK2-related pathway would be activated in the presence of overexpressed MFAP3L. To address this question, we established two stable SW480 cell lines with overexpression of the dominant-positive mutant (DP; Y287D) and the dominant-negative mutant (DN; Y287A) of MFAP3L. Then, we conducted a comparison experiment in EV+, MF+, DP and DN cells to examine the activation status of the ERK2 pathway and the expression status of the genes regulated by the ERK2 pathway. The phosphorylation status of ELK1 was selected as a marker of the activated ERK2 pathway. As shown in Fig. 5a, compared with the other studied cells, DP cells showed the highest phosphorylation levels of ERK2 and ELK1 and the highest levels of cathepsin D, MMP2 and osteopontin, which are commonly up-regulated by the ERK pathway during metastasis [11,16,19,20]. In contrast to EV+ cells, a remarkably higher phosphorylation level of ELK1 and expression level of cathepsin D, MMP2 and osteopontin was detected in MF+ cells, likely due to ERK2 phosphorylation, whereas these biological events were not observed in the DN cells, as the Y287A mutant cannot phosphorylate ERK2 and activate the ERK pathway. Correspondingly, in Transwell assays, the DP cells displayed the highest invasion capacity compared with the other cell types, while MF+ cells exhibited a relatively higher invasion capacity than EV+ and DN cells (Fig. 5b, $p < 0.001$). These results indicate that pTyr287 of MFAP3L is required for its kinase activity and activation of the ERK pathway. Moreover, the activation of the ERK pathway in the nucleus induced by MFAP3L highly correlated with the invasion capacity of the cancer cells. In addition, when ERK2 expression was knocked-down through RNAi in DP cells, ERK2 phosphorylation and the invasion capacity of the DP cells were dramatically attenuated (Fig. 5c and d; $p < 0.001$). This experimental evidence led us to conclude that MFAP3L significantly activates the ERK2 pathway; in turn, ERK2 phosphorylation promotes a higher expression of metastasis-related genes, resulting in CRC metastasis and invasion.

ERK2 phosphorylation and activation are generally induced by EGF through EGFR and the cytoplasmic RAS/RAF/MEK pathway, with transient responses observed within a period of less than 1 h [18]. Because MFAP3L is phosphorylated by nuclear EGFR, and ERK2 is a phosphorylation substrate of EGFR signaling or MFAP3L (Fig. 3c), we analyzed the contribution of MFAP3L to ERK2 activation. In EV+ cells, which showed lower MFAP3L expression, the signal for ERK2 phosphorylation was temporarily enhanced by EGF treatment and attenuated within 1 h. However, in MF+ cells, which showed a higher abundance of MFAP3L, pERK2 was clearly increased within 30 min, without attenuation for at least 1 h (Fig. 3c). Therefore, under EGF/EGFR induction, MFAP3L is likely

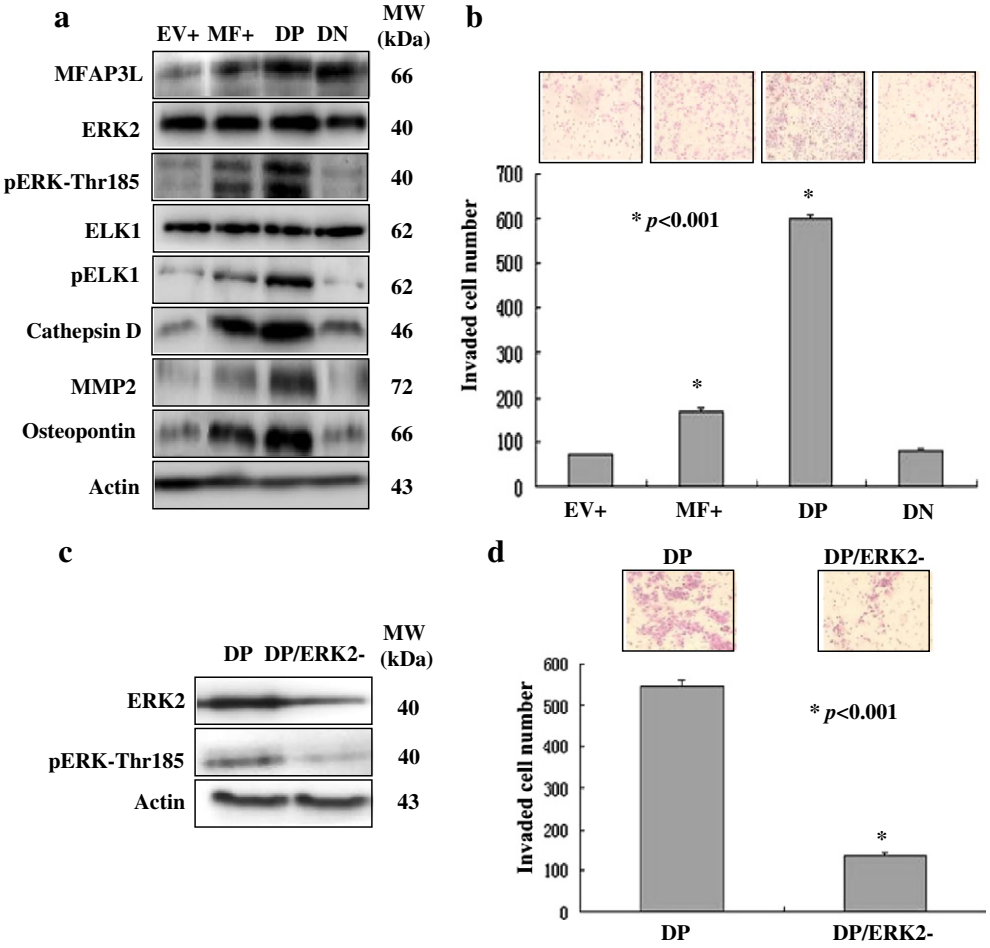

Fig. 5. *MFAP3L activates the ERK2 cascade and enhances the invasion of colon cancer cells.* a, Western blot analysis to determine the activation status of the ERK pathway in EV+, MF+, DP and DN cells. b, d, Transwell invasion assay using EV+, MF+, DP and DN cells, DP cells with transient ERK2 RNAi (DP/ERK2-) and control cells. For the Transwell assay, ten fields of view were counted, and three independent experiments were performed to calculate the average. c, Western blot analysis to determine whether the ERK pathway was inhibited by transient ERK2 RNAi in DP cells.

to maintain its stimulation signals for a longer period of time by effectively converting dephosphorylated ERK2 to pERK2 in the nucleus.

4. Discussion

In this study, we provided evidence that MFAP3L is a novel member of the nuclear EGFR signaling pathway and possesses protein kinase activity that can phosphorylate ERK2 at Thr185 and Tyr187. Accordingly, MFAP3L phosphorylation in the nucleus is an important inducer that enhances CRC invasion and metastasis. Due to its nuclear localization and the enhanced expression and phosphorylation of MFAP3L in CRC tissues and cells, this new protein kinase may be considered a novel protein biomarker, especially regarding the application of antibodies targeting MFAP3L for IHC analysis. In addition, EGFR inhibitors are widely used in therapies for cancer, including CRC. Based on our observation, MFAP3L is likely to play a key role in nuclear EGFR signaling, and the regulation of MFAP3L kinase activity may therefore have pharmaceutical effects on tumor progression.

Based on NCBI Blast results, MFAP3L showed 71% homology to microfibrillar-associated protein 3 (MFAP3). Further alignment analysis revealed that these two proteins demonstrate poor homology with any other known protein, including the other members of the MAGP family, which are components of microfibrils in the extracellular matrix of many tissues [21]. Thus, MFAP3L may function differently from other members of the MAGP family. Based on our bioinformatic analysis and experiments with MFAP3L protein, we noted several interesting observations. For instance, although the bioinformatic analysis predicted that MFAP3L contains a single-pass transmembrane domain, our experimental results indicated that this protein was not located at the plasma membrane but was rather primarily in the nucleus. Because nuclear proteins generally display hydrophobic features, the potential transmembrane domain of MFAP3L may facilitate its interactions with components of the nuclear membrane. Our bioinformatic analysis further predicted that MFAP3L contains protein sequences similar to those commonly found in the catalytic domains of protein kinases, although MFAP3L does not possess an intact classical catalytic domain. Our experimental results, nevertheless, demonstrated that MFAP3L indeed had kinase activity against ERK2. Thus, further investigation is necessary to gain a deeper understanding of the relationship between the protein structure and enzymatic activity of MFAP3L, as our findings may reveal a novel catalytic domain that differs from that of known kinases. Furthermore, our bioinformatic analysis indicated that there is a conserved SH2 motif with a potential EGFR phosphorylation site at Tyr287. This theoretical analysis correlated with the experimental evidence described above, in which nuclear-translocated EGFR phosphorylated MFAP3L at Tyr287 and activated its kinase activity. Together, these findings suggest that MFAP3L is a novel mediator of EGFR nuclear signaling.

According to previous studies, certain transcription factors (TFs) can be phosphorylated by different kinases, leading to their shuttling between the cytoplasmic and nuclear compartments. For example, similar to the cytoplasmic kinase PKA, the nuclear kinase MSK1 is also

able to phosphorylate NFκB at Ser276 upon TNF stimulation, and this phosphorylation results in the selective transcriptional activation of NFκB [22]. It is also well known that cytoplasmic ERK is activated by the RAS/RAF pathway through the phosphorylation of certain threonine and tyrosine residues in its TXY motif [16]. Phosphorylated ERK translocates to the nucleus and, in turn, activates downstream TFs, such as ELK1 and c-fos. Consequently, the overexpression of certain genes promotes cell proliferation, survival and invasion [16,18]. The nuclear export of dephosphorylated ERK is dependent on the dephosphorylation process regulated by the specific phosphatase MKP in the nucleus [23]. The rapid turnover of phosphorylation and dephosphorylation thus results in the dynamic shuttling of ERK between the nuclear and cytoplasmic compartments [24]. In this study, we introduce a novel nuclear kinase, MFAP3L, which may play an active role in the phosphorylation of nuclear ERK at Thr185 and Tyr187. Under EGF stimulation, MFAP3L was phosphorylated and activated, and activated MFAP3L further reacted with nuclear ERK2. Consequently, these chain phosphorylations may alter ERK2 shuttling and impact cell survival and invasion. With this kinase activity of MFAP3L, ERK phosphorylation and function would be expected to be more efficient. Therefore, identification of MFAP3L localization as well as its function is likely to unveil an alternative activation system of ERK in the nucleus and offer clues regarding how this nuclear kinase regulates transcription. Although there are many reports regarding the translocation of EGFR into the nucleus in a ligand-dependent manner [25,26] and showing that this translocation is accompanied by gene expression resulting in phenotypic changes in cancer cells [11,13], the molecular mechanisms underlying this process are extremely limited but are either related to nuclear import or nuclear signal transduction [12,26]. Based on our observations, activation of the MFAP3L kinase likely helps to regulate multiple functions of nuclear-translocated EGFR in colon cancer cells. The accumulated EGFR in the nucleus directly phosphorylates MFAP3L at Tyr287, and phosphorylated MFAP3L transduces the activation signal to its substrate ERK2, subsequently promoting cancer cell invasion and metastasis. As a novel mediator, MFAP3L directly connects EGFR to the downstream ERK pathway in the nucleus without detouring through other pathways, such as the classical RAS/RAF/MEK pathway. Therefore, the coupling of signaling transduction between EGFR and MFAP3L constitutes an alternative activation system for ERK in the nucleus, which regulates tumor progression and differs from that of the cytoplasmic EGFR pathway.

Conflicts of interest

The authors declare no conflicts of interest.

Acknowledgments

This work was supported by the National High Technology Research and Development Program of China (2012AA020206) and the Major State Basic Research Development Program of China (2009CB522200). We are grateful to Dr. Wei Zhao from the Beijing Cancer Hospital for the confocal microscopy assessment and Dr. Xiaozhong Peng from the Institute of Basic Medical Sciences, Chinese Academy of Medical Sciences for the autoradiography experiment.

References

[1] R.Y. Haig, M. Merne, A. Hansson, X. Zheng, K. Roberg, M. Nees, K. Iljin, B.K. Bloor, P.R. Morgan, B. Fadeel, R.C. Grafström, Differentiation-promoting culture of competent and noncompetent keratinocytes identifies biomarkers for head and neck cancer, Am. J. Pathol. 180 (2011) 457–472.
[2] A.R. Albig, D.J. Becenti, T.G. Roy, W.P. Schiemann, Microfibril-associate glycoprotein-2 (MAGP-2) promotes angiogenic cell sprouting by blocking notch signaling in endothelial cells, Microvasc. Res. 76 (2008) 7–14.
[3] S.C. Mok, T. Bonome, V. Vathipadiekal, A. Bell, M.E. Johnson, K.K. Wong, D.C. Park, K. Hao, D.K. Yip, H. Donninger, L. Ozbun, G. Samimi, J. Brady, M. Randonovich, C.A. Pise-Masison, J.C. Barrett, W.H. Wong, W.R. Welch, R.S. Berkowitz, M.J. Birrer, A gene signature predictive for outcome in advanced ovarian cancer identifies a survival factor: microfibril-associated glycoprotein 2, Cancer Cell 16 (2009) 521–532.
[4] K.A. Spivey, J. Banyard, A prognostic gene signature in advanced ovarian cancer reveals a microfibril-associated protein (MAGP2) as a promoter of tumor cell survival and angiogenesis, Cell Adhes. Migr. 4 (2010) 169–171.
[5] B. Kang, C. Hao, H. Wang, J. Zhang, R. Xing, J. Shao, W. Li, N. Xu, Y. Lu, S. Liu, Evaluation of hepatic-metastasis risk of colorectal cancer upon the protein signature of PI3K/AKT pathway, J. Proteome Res. 7 (2008) 3507–3515.
[6] J.H. Wu, X.Y. Tian, C.Y. Hao, The significance of a group of molecular markers and clinicopathological factors in identifying colorectal liver metastasis, Hepatogastroenterology 58 (2011) 1182–1188.
[7] J. Xiao, L. Yin, J. Li, H. Zu, Z. Zhou, B. Zhao, J. Sha, Molecular cloning, identification and characteristics of NYD-SP9: gene coding protein kinase presumably involved in spermatogenesis, Chin. Sci. Bull. 47 (2002) 896–901.
[8] A. Wells, Tumor invasion: role of growth factor-induced cell motility, Adv. Cancer Res. 78 (2000) 31–101.
[9] A. Citri, Y. Yarden, EGF–ERBB signalling: towards the systems level, Nat. Rev. Mol. Cell Biol. 7 (2006) 505–516.
[10] H. Cao, Z.M. Lei, L. Bian, C.V. Rao, Functional nuclear epidermal growth factor receptors in human choriocarcinoma JEG-3 cells and normal human placenta, Endocrinology 136 (1995) 3163–3172.
[11] A. Psyrri, Z. Yu, P.M. Weinberger, C. Sasaki, B. Haffty, R. Camp, D. Rimm, B.A. Burtness, Quantitative determination of nuclear and cytoplasmic epidermal growth factor receptor expression in oropharyngeal squamous cell cancer by using automated quantitative analysis, Clin. Cancer Res. 11 (2005) 5856–5862.
[12] S.Y. Lin, K. Makino, W. Xia, A. Matin, Y. Wen, K.Y. Kwong, L. Bourguignon, M.C. Hung, Nuclear localization of EGF receptor and its potential new role as a transcription factor, Nat. Cell Biol. 3 (2001) 802–808.
[13] H.W. Lo, W. Xia, Y. Wei, M. Ali-Seyed, S.F. Huang, M.C. Hung, Novel prognostic value of nuclear epidermal growth factor receptor in breast cancer, Cancer Res. 65 (2005) 338–348.
[14] C.A. Zampieri, J.F. Fortin, G.P. Nolan, G.J. Nabel, The ERK mitogen-activated protein kinase pathway contributes to Ebola virus glycoprotein-induced cytotoxicity, J. Virol. 81 (2007) 1230–1240.
[15] H.W. Lo, S.C. Hsu, M. Ali-Seyed, M. Gunduz, W. Xia, Y. Wei, G. Bartholomeusz, J.Y. Shih, M.C. Hung, Nuclear interaction of EGFR and STAT3 in the activation of the iNOS/NO pathway, Cancer Cell 7 (2005) 75–89.
[16] G. Pearson, F. Robinson, T. Beers Gibson, B.E. Xu, M. Karandikar, K. Berman, M.H. Cobb, Mitogen-activated protein (MAP) kinase pathways: regulation and physiological functions, Endocr. Rev. 22 (2001) 153–183.
[17] J.W. Haycock, Peptide substrates for ERK1/2: structure-function studies of serine 31 in tyrosine hydroxylase, J. Neurosci. Methods 116 (2002) 29–34.
[18] J.W. Lee, R. Juliano, Mitogenic signal transduction by integrin- and growth factor receptor-mediated pathways, Mol. Cells 17 (2004) 188–202.
[19] Y. Okada, G. Eibl, S. Guha, J.P. Duffy, H.A. Reber, O.J. Hines, Nerve growth factor stimulates MMP-2 expression and activity and increases invasion by human pancreatic cancer cells, Clin. Exp. Metastasis 21 (2004) 285–292.
[20] S. Silletti, M. Yebra, B. Perez, V. Cirulli, M. McMahon, A.M. Montgomery, Extracellular signal-regulated kinase (ERK)-dependent gene expression contributes to L1 cell adhesion molecule-dependent motility and invasion, J. Biol. Chem. 279 (2004) 28880–28888.
[21] A. Miyamoto, R. Lau, P.W. Hein, J.M. Shipley, G. Weinmaster, Microfibrillar proteins MAGP-1 and MAGP-2 induce Notch1 extracellular domain dissociation and receptor activation, J. Biol. Chem. 281 (2006) 10089–10097.
[22] L. Vermeulen, G. De Wilde, P. Van Damme, W. Vanden Berghe, G. Haegeman, Transcriptional activation of the NF-kappaB p65 subunit by mitogen- and stress-activated protein kinase-1 (MSK1), EMBO J. 22 (2003) 1313–1324.
[23] J.M. Brondello, A. Brunet, J. Pouyssegur, F.R. McKenzie, The dual specificity mitogen-activated protein kinase phosphatase-1 and -2 are induced by the p42/p44MAPK cascade, J. Biol. Chem. 272 (1997) 1368–1376.
[24] M. Costa, M. Marchi, F. Cardarelli, A. Roy, F. Beltram, L. Maffei, G.M. Ratto, Dynamic regulation of ERK2 nuclear translocation and mobility in living cells, J. Cell Sci. 119 (2006) 4952–4963.
[25] G. Carpenter, Nuclear localization and possible functions of receptor tyrosine kinases, Curr. Opin. Cell Biol. 15 (2003) 143–148.
[26] J. Schlessinger, M.A. Lemmon, Nuclear signaling by receptor tyrosine kinases: the first robin of spring, Cell 127 (2006) 45–48.